Inhibition of the Fusion-Inducing Conformational Change of Influenza Hemagglutinin by Benzoquinones and Hydroquinones†

Dale L. Bodian,‡,§ R. Bryan Yamasaki,‖ Richard L. Buswell,‖ Jay F. Stearns,‖ Judith M. White,‡,⊥ and I. D. Kuntz*,‡,#

Department of Biochemistry and Biophysics, University of California, San Francisco, San Francisco, California 94143-0448, Department of Pharmaceutical Chemistry, University of California, San Francisco, San Francisco, California 94143-0446, Department of Pharmacology, University of California, San Francisco, San Francisco, California 94143-0450, and Seres Laboratories, Inc., 3331 Industrial Drive, Santa Rosa, California 95403

Received September 1, 1992

ABSTRACT: Influenza hemagglutinin (HA) undergoes a conformational change that is required for viral entry. The rearrangement includes exposure of the fusion peptide, a hydrophobic segment buried in the trimer interface of the native protein. Since fusion peptide release triggers the membrane fusion event crucial for viral replication, inhibition of fusion peptide exposure should prevent infection. We reasoned that small molecules that bind to HA and stabilize its nonfusogenic conformation would block viral activity. A computer-assisted method was used to select putative HA ligands. One of the selected compounds, 4A,5,8,8A-tetrahydro-5,8-methano-1,4-naphthoquinone, prevented the conversion of X31 HA to a conformation recognized by α-fusion peptide antisera. Several derivatives of this compound, including both benzoquinones and hydroquinones, also showed inhibition. The most effective compounds tested have IC_{50}s between 1 and 20 μM. Representative compounds also inhibited virus-induced syncytia formation, HA-mediated hemolysis, and viral infectivity in vitro. The inhibitors are attractive leads for the development of antiviral drugs and can serve as probes of the mechanism of the conformational change of HA.

Influenza is an enveloped virus and must fuse with a host cell in order to replicate [for reviews, see Stegmann et al. (1989), White (1990), and Wiley and Skehel (1987)]. Fusion is pH-dependent and occurs in the host cell endosome. Fusion between the membrane of the virus and the endosomal membrane is mediated by hemagglutinin (HA),[1] a trimeric glycoprotein integral to the viral membrane (Wiley & Skehel, 1987). The identical monomers of HA are composed of two disulfide-linked polypeptide chains, HA1 and HA2. A hydrophobic sequence at the N terminus of HA2, the fusion peptide, is directly involved in promoting fusion.

The structure of the ectodomain of the trimer (BHA) has been determined crystallographically (Wilson et al., 1981). The three-dimensional structure has been described as comprising three domains: a stem region proximal to the membrane, a globular head domain possessing receptor binding activity, and a connecting hinge region. In the native form of HA, the fusion peptide is buried in the trimer interface in the stem region. The fusion peptide is released from its unexposed location by a pH-triggered irreversible conformational change that is a prerequisite for fusion [for reviews, see Stegmann et al. (1989), White (1990), and Wiley and Skehel (1987)].

Since exposure of the fusion peptide is required for fusion, inhibition of its release should prevent viral replication. Thus, one possible antiviral strategy is to identify a small molecule that binds to the nonfusogenic form of HA and stabilizes that conformation over all fusogenic conformations. A structure-based method has been used to identify a putative binding site for such an inhibitor and to select candidate ligands.

MATERIALS AND METHODS

Cells and Media. CV-1 cells (American Type Tissue Culture Collection) were maintained in CV-1 growth media [Dulbecco's minimal essential media (DME), 10% supplemented bovine calf serum (SCS), 2 mM glutamine, 100 units/mL penicillin, and 100 mg/mL streptomycin (pen/strep)]. MDCK2 (Madin-Darby canine kidney) cells, a gift of Dr. Barry Gumbiner, were grown in MDCK growth media [MEM–EBSS (minimal essential media with Earle's balanced salt solution), 5% SCS, 2 mM glutamine, pen/strep, 25 mM HEPES (*N*-(2-hydroxyethyl)piperazine-*N*′-2-ethanesulfonic acid) pH 7.2]. Wt-HA-expressing CHO-DUKX cells (Wtm8005 cell line), a gift of Dr. Don Wiley, were maintained in G418 media (MEM-α without nucleosides, 10% SCS, 2 mM glutamine, pen/strep, 600 μg/mL geneticin, 0.3 μM methotrexate). Unless otherwise noted, all tissue culture reagents were obtained from the UCSF Cell Culture Facility.

† This work was supported by NIH Grants AI-28126, GM-31497 (I.D.K.), AI-22470 (J.M.W.), and GM-39552 (G. L. Kenyon, principal investigator), training Grant GM-08120, and an NSF predoctoral fellowship (D.L.B.).

* Corresponding author.

‡ Department of Biochemistry and Biophysics, University of California, San Francisco.

§ Current address: Laboratory of Molecular Biophysics, South Parks Road, University of Oxford, Oxford OX1 3QU, U.K.

‖ Seres Laboratories, Inc.

⊥ Department of Pharmacology, University of California, San Francisco.

Department of Pharmaceutical Chemistry, University of California, San Francisco.

[1] Abbreviations: HA, hemagglutinin; BHA, ectodomain of hemagglutinin generated by bromelain cleavage; PDB, Protein Data Bank; FCD, Fine Chemicals Directory; SPA, scintillation proximity assay; EIA, ELISA-based infectivity assay; DMSO, dimethyl sulfoxide; cpm, counts per minute; FDQ, fluorescence dequenching; R_{18}, octadecyl rhodamine; MES, 2-(*N*-Morpholino)ethanesulfonic acid; HEPES, *N*-(2-hydroxyethyl)piperazine-*N*′-2-ethanesulfonic acid; NP40, Nonidet-P40; pen/strep, penicillin and streptomycin; PBS, phosphate-buffered saline; MEM, minimal essential media; DME, Dulbecco's minimal essential media; SCS, supplemented bovine calf serum; FBS, fetal bovine serum.

0006-2960/93/0432-2967$04.00/0

Antibodies. Drs. Richard Lerner and Ian Wilson of Scripps provided α-fusion peptide antiserum raised against residues 1–29 of HA2. The data presented were obtained with this antibody while preliminary experiments employed antisera raised against residues 1–15 of HA2. The site A mouse monoclonal antibody was the gift of Dr. John Skehel.

Synthesis, Purification, and Characterization of Test Compounds. 2,6,6-Trimethyl-2-cyclohexene-1,4-dione (84) was purchased from Fluka. 1,4-naphthoquinone (90), 2,3-dimethylhydroquinone (99), 4-chloro-1-naphthol (101), quinizarin (102), 2,3-dicyanohydroquinone (103), hydroquinone (104), phthalhydrazide (108), *tert*-butylhydroquinone (117), 2-methyl-1,4-naphthoquinone (118), 5-hydroxy-1,4-naphthoquinone (119), 2-hydroxy-1,4-naphthoquinone (120), 4-amino-1-naphthol hydrochloride (121), and 1,5-naphthalenediol (126) were purchased from Aldrich. 3′,6′-Dihydroxybenzonorbornane (111) was from TCI. 1,4-Anthraquinone (114) was from Lancaster Synthesis. 4A,5,8,8A-Tetrahydro-5,8-methano-1,4-naphthoquinone (83) and 2,5-dimethylhydroquinone (116) were from Pfaltz and Bauer and 5,8-dioxo-1,4,4A,5,8,8A-hexahydro-1-naphthalene carboxylic acid (91) from Bader. Recrystallization of 83 from hexane yielded 83K. 5,8-Dihydro-5,8-methano-1,4-naphthalenediol (83A) was prepared from 83K by the method of Porter et al. (1964). 2-Bromo-1,4-naphthoquinone (135) was prepared following a published procedure (Grunwell et al., 1991) and then further purified by sublimation. Prior to screening, compounds 90, 119, 120, and 126 were recrystallized and 99, 114, and 116 were purified by sublimation. Structures of all compounds except 91 and 135 were confirmed by ^{1}H NMR. Structures of compounds 83A and 83K were also confirmed by mass spectrometry and IR. All compounds except 91 passed elemental analysis within experimental error; 121 passed as $^1/_4$ H_2O. Melting points of all compounds except 91 and 121 agreed with published values. TLC analysis of compound 91 revealed it to be a complex mixture. Stock solutions of all compounds were made fresh daily in DMSO.

Virus and Protein. Inoculum for X31 influenza virus (H3N2) was the plaque-purified subtype C22 (Doms et al., 1986), a gift of Dr. Ari Helenius. Virus was propagated in fertilized chicken embryos and purified as previously described (Skehel & Schild, 1971). [^{3}H-Leu]BHA was metabolically labeled following the published procedure for [^{35}S-Met]HA (White & Wilson, 1987) except that Leu$^-$ media (MEM, 2.2 g/L $NaHCO_3$, 58 mg/L lysine, 15 mg/L methionine, pH 7.3) was used in place of Met$^-$ media, and infected cells were labeled with 0.5 mCi/flask [3,4,5-^{3}H]leucine (NEN). Bromelain cleavage and purification of BHA were carried out as described (Doms et al., 1985).

Scintillation Proximity Assay (SPA). [^{3}H-Leu]BHA was diluted to 10 000 cpm/200 μL in MSSH buffer [10 mM HEPES, 10 mM MES (2-(*N*-morpholino)ethanesulfonic acid), 10 mM succinate, 0.10 M NaCl, pH 7.0] and 0.1% NP40 (Nonidet P40). Protein was incubated with the specified concentration of trial compound for 25 min at room temperature. The concentration of DMSO in all reactions was 0.67% (v/v). A predetermined amount of acetic acid was added to bring the reactions to pH 5.0, unless otherwise noted. Following a 5-min incubation at room temperature, reactions were reneutralized with NaOH. For POST controls, compounds were added after reneutralization. Aliquots (200 μL) of the protein solutions were then mixed with 100 μL of protein A-SPA beads (Amersham) suspended in MSSH buffer, 5% fetal bovine serum (FBS), and 1 μL of fusion peptide antiserum in 50% glycerol and incubated overnight at room temperature with constant shaking. Counts per minute were detected in a Beckman LS3801 scintillation counter without addition of liquid scintillant.

To compute the IC_{50} for each compound, the cpm detected in identical samples were averaged. The reduction in cpm due to nonspecific quenching was calculated as $F_c = cpm_{POST}/cpm_{DMSO}$, where cpm_{POST} is the number of cpm detected in the POST control, and cpm_{DMSO} is the number of cpm detected in samples with test compound omitted. The cpm per sample corrected for nonspecific quenching was computed as $cpm_{corr} = cpm_{obs}/F_c$, where cpm_{obs} is the observed cpm in the samples containing the trial compound. Inhibition was then calculated as percent inhibition = $(cpm_{DMSO}-cpm_{corr})/cpm_{DMSO} \times 100\%$. The percent inhibition was plotted as a function of the log of the concentration of compound, and the IC_{50}, the concentration eliciting half-maximal inhibition, was estimated from the graph.

Dilution Experiment. [^{3}H-Leu]BHA at 1000 cpm/μL in MES saline (0.13 M NaCl, 20 mM MES, pH 7.0) and 0.1% NP40 was incubated with 1 mM compound or DMSO alone. The concentration of DMSO was 2.2% (v/v). After incubation for 2 h at room temperature, the samples were diluted 25-fold with MES saline/0.1% NP40 containing either 1 mM compound or DMSO alone. Samples were incubated a further 2 h and then acidified to pH 5.0 for 5 min at room temperature. Following reneutralization, compound (POST control) or DMSO alone was added to each sample. Reactions were subjected to SPA analysis as described above.

pH Control. Acidification reactions were identical to those performed for SPA analysis, except detergent and radiolabeled protein were omitted. The pH of acidified compound-containing solutions was compared to that of an identical solution containing DMSO but without test compound.

Hemagglutination. Hemagglutination experiments were done by standard methods (WHO Collaborating Centers for Reference and Research on Influenza, 1982). For testing compounds for inhibition of hemagglutination, virus in PBS was incubated for 30 min at room temperature with double the concentration of ligand. Serial dilutions of virus were made in a solution of PBS containing twice the desired final concentration of compound. An equal volume of 0.5% human red blood cells (rbcs) was then added and allowed to agglutinate.

Hemolysis. Hemolysis experiments were based on a previously described protocol (Doms et al., 1986). Human red blood cells (used within 1–2 days) were washed twice with PBS and then suspended to 1% (v/v) with MES saline. Virus titrations determined that 0.6 μg of viral protein (estimated by the procedure of Lowry) gave an OD in the center of the linear range. Virus and compound were preincubated for 0.5 h at room temperature in a volume of 100 μL. The DMSO concentration was identical in all samples in a given experiment. Three hundred fifty microliters of 1% washed red blood cells was added, and the reaction was warmed to 37 °C for 5 min. The pH was lowered to 5.0 (unless otherwise noted) by addition of a predetermined amount of 1 N acetic acid. After incubation for 15 min at 37 °C, the reaction was reneutralized with NaOH. Intact red blood cells were pelleted by centrifugation at 10 000*g* for 3 min. The OD_{570} was measured on 150-μL aliquots of supernatant. Background values were determined from identically treated samples lacking virus. Control samples measuring the quenching of OD_{570} by the compounds were identical to other reactions except that virus was replaced by the same volume of assay

buffer and red blood cells were prelysed in 10 mM MES, pH 7.

To compute the IC_{50}, the percent reduction in OD of samples containing compounds were calculated as

$$\left[1 - \frac{(OD_{DMSO,-} - OD_{DMSO,+})}{(OD_{-} - OD_{+})}\right] \times 100\%$$

where $OD_{DMSO,+}$ is the absorbance of samples containing DMSO, $OD_{DMSO,-}$ is the background lysis of red blood cells without virus present but with DMSO, OD_{+} is the absorbance of the compound- and virus-containing samples, and OD_{-} is the OD of samples containing compound but no virus. The percent reduction of OD of the control samples with prelysed red blood cells was subtracted from each value. The IC_{50} is defined as the concentration reducing the OD by the same amount as samples containing half the amount of virus. Depending on the day, 50% less virus reduced the OD by 25–60%.

Fluorescence Dequenching Fusion Assay. Octadecyl rhodamine (R_{18}) was incorporated into the membranes of red blood cells following a previously published protocol (Morris et al., 1989). Binding of labeled red blood cells to HA-expressing cells and fusion reactions were carried out as described (Kemble et al., 1992). Compounds or DMSO were incubated with the cell–red blood cell complexes for 5–20 min at 37 °C prior to initiation of the fusion reaction.

Syncytia Formation. Influenza-mediated cell–cell fusion was induced following the previously described protocol for fusion from without (Doms et al., 1986). CV-1 cells were plated in six-well cluster dishes at 150 000 cells per well and then grown for 1 day in CV-1 growth media. Cells were washed once with ice cold PBS. A total of 1 mL of DME, supplemented with pen/strep, with or without 6.5 μg of virus (protein concentration determined by the method of Lowry) and the appropriate concentration of trial compound was added to each well on ice. The final concentration of DMSO in all wells was 0.1% by volume. After binding at 4 °C for 1 h, the virus solution was aspirated and replaced with prewarmed MSSH buffer, pH 5.2, containing the same concentrations of compound and DMSO. The buffer was aspirated after incubation at 37 °C for 3 min. Cells were allowed to recuperate in CV-1 growth media without compounds for 4 h. Cells were examined for any alterations in cell morphology, stained for 30 min at room temperature with 0.2% crystal violet in 50% ethanol, and photographed with an Olympus IMT-2 microscope.

CV-1 Viability Test. CV-1 cells were plated in 96-well tissue culture dishes at 10 000 cells per well and grown in CV-1 growth media for 24 h. The appropriate concentration of compound in DME and pen/strep was added and incubated for 1 h at 4 °C with constant agitation. The total concentration of DMSO in all wells was 0.6%. Following the binding period, cells were examined for any observable changes in morphology. Cells were rinsed twice with PBS and then incubated with 25 μL of 2 mg/mL MTT in PBS and 50 μL of DME and pen/strep. Plates were incubated and processed for spectrophotometry as described under MTT Viability Assay below.

EIA Antiviral Assay. MDCK2 cells were seeded at 35 000 cells per well in 96-well plates and grown in MDCK growth media for 24 h at 37 °C, under 5% CO_2. C22 virus was preincubated with the appropriate concentration of test compound in MEM-EBSS with pen/strep for 25 min at room temperature. All samples were performed in triplicate and contained 0.67% (v/v) DMSO and 0.0–1.5 hemagglutinating units of virus. Cells were infected in the presence of test compounds for 15 h at 37 °C, under 5% CO_2. Cells were rinsed once with PBS and then fixed with 80% acetone/PBS for 15 min at room temperature and allowed to air dry. Plates were washed with PBS/0.05% Tween 20 and then blocked with EIA diluent (PBS, 1% FBS, 0.1% Tween 20) for 30 min at room temperature. Wells were incubated with site A monoclonal antibody (diluted to 1:2000 with EIA diluent) for 1 h at 37 °C, washed four times with PBS/0.05% Tween 20, and then incubated for 1 h at 37 °C with F(ab)′-2-goat-anti-mouse Ig(G)–peroxidase (Boehringer Mannheim) (diluted to 1:6000 with EIA diluent). Plates were washed four times with PBS/0.05% Tween 20. A 0.3 mg/mL solution of 3,3′,5,5′-tetramethylbenzidine substrate was prepared in citrate–acetate buffer (0.1 M sodium acetate brought to pH 5.5 with 1.0 M citric acid) with 6% (v/v) DMSO and 0.005% H_2O_2. Color development proceeded for 10 min at room temperature and then was stopped by the addition of 2 M sulfuric acid. The OD in each well was read at 410 nm on a Dynatech microtiter plate reader.

Each trial compound was tested with at least two different concentrations of virus. A standard curve relating the amount of infecting virus to OD_{410} was determined from virus titrations without test compounds on each plate. Inhibition was computed as the percent reduction of infectious virus producing the OD_{410} observed in the compound containing wells. The results from all concentrations of virus producing ODs in the linear range from independent experiments were averaged. The percent inhibition was plotted as a function of log concentration for each compound. The IC_{50}, the concentration at which 50% inhibition was observed, was taken from the graph.

MTT Viability Assay. MDCK2 cells were infected with virus, compounds, and DMSO as described above. Following the 15-h incubation, cells were washed twice with PBS to remove the test compounds. The viability assay was conducted as described (Mosmann, 1983) except that 50 μL of MDCK2 growth media and 25 μL of 2 mg/mL 3-(4,5-dimethylthiazol-2-yl)-2,5-diphenyltetrazolium bromide in PBS were added to each well. The OD_{570} for each well was read on a microtiter plate reader. The ODs from identical wells were averaged, and the percent inhibition was computed by comparison to the average OD of wells containing DMSO but no trial compound. The CC_{50}, the concentration at which 50% of the cells were viable, was estimated from a plot of log concentration vs percent inhibition.

Computer Modeling: Site Selection and Docking. The structure-based inhibitor design method, DOCK, identifies a potential binding site on a protein of interest (the "receptor") and then selects small molecules likely to bind to the site (DesJarlais et al., 1988; Kuntz et al., 1982; Shoichet et al., 1992). The component programs SPHGEN, CLUSTER, DISTMAP, and DOCK2 have been described in detail elsewhere (DesJarlais et al., 1988; Kuntz et al., 1982; Shoichet et al., 1992). Briefly, the inhibitor discovery process begins with a calculated molecular surface representing the solvent-accessible regions of the receptor (Richards, 1977). SPHGEN searches the surface for concave regions and characterizes each cavity as a set of overlapping spheres. Each set, or "cluster", represents a possible binding site for a small molecule. The user selects a single cluster best satisfying the requirements of the particular application. Typically, only clusters of at least 15 spheres are considered.

The cluster definition is then used by the DOCK2 program to identify ligands with shapes complementary to that of the target site. DOCK2 searches a database containing three-

Table I: Input Parameters for the Computer Programs SPHGEN, CLUSTER, DISTMAP, and DOCK2[a]

I SPHGEN		II CLUSTER		III DISTMAP		IV DOCK2		V DISTMAP		VI DOCK2	
variable	value	variable	value	variable	value	variable	value	variable	value	variable	value
dentag	X	*maxrad*	5.0	*polcon*	2.3	*dislim*	1.5	*polcon*	2.4	*dislim*	1.5
dotlim	0.0	*m2xrad*	0	*ccon*	2.6	*nodlim*	5	*ccon*	2.8	*nodlim*	5
radmax	5.0	*povlap*	0	*discut*	4.5	*ratiom*	0.0	*discut*	4.5	*ratiom*	0.0
		clusiz	250	*maxgrid*	3	*lownod*	4	*maxgrid*	4	*lownod*	4
		minsiz	1			*lbinsz*	0.15			*lbinsz*	0.15
		minflg	0			*lovlap*	0.0			*lovlap*	0.0
		yn	y			*sbinsz*	1.0			*sbinsz*	1.0
		minrad	1.0			*sovlap*	0.0			*sovlap*	0.0
		rincr	0.5			*nbump*	0			*nbump*	0
		nearnb	0.5			*natmin*	10			*natmin*	10
		nearad	0.25			*natmax*	60			*natmax*	35
						expmax	0			*expmax*	1
										fctbmp	1

[a] The variables are defined in the DOCK user's manual and described in previous publications (DesJarlais et al., 1988; Kuntz et al., 1982; Shoichet et al., 1992).

dimensional coordinates of small molecules and docks each molecule into the site by mapping ligand atoms onto sphere centers. Both the ligand and receptor are treated as rigid during this process. Each molecule in the database is tested in thousands of configurations in the site and each configuration is scored by a function approximating a van der Waals energy. High scores are assigned to ligands with extensive favorable contacts with site atoms. In DOCK2, potential electrostatic and hydrogen-bonding interactions are evaluated visually by the user. The best candidate inhibitors are then screened experimentally.

To apply DOCK to HA, atomic coordinates of X31 BHA (Wilson et al., 1981) were obtained from entry 1hmg of the Brookhaven Protein Databank (Abola et al., 1987; Bernstein et al., 1977). This crystal structure has a resolution of 3 Å. The molecular surface (Richards, 1977) was computed for the stem region of a single monomer, residues 1–39 and 315–328 of HA1 and 1–50 and 100–175 of HA2, in the context of the entire trimer. The surface was generated at a density of 5.4 points/Å^2 with a 1.4-Å radius probe sphere. Carbohydrate residues and water molecules were excluded from the calculation. Potential binding sites were identified by running SPHGEN on the surface with the parameters listed in Table I, column I. A total of 23 clusters with at least 15 spheres were found in 5 h 43 min of cpu time on a VAX 8650. The site represented by the largest cluster was selected. However, this cluster contained spheres in shallow ridges well beyond the edge of the central, deepest site. Manual elimination of the spheres included in the original cluster due to overlaps with large spheres gave a 54-sphere cluster. Ligands with shape complementarity to the target site were identified by docking small molecules to this cluster using the DOCK2 program. Scores were precalculated on a grid over the receptor site with the program DISTMAP. Input parameters for DISTMAP and DOCK2 are listed in Table I, columns III and IV. Docking 55 000 compounds took approximately 330 h on an IRIS 4D/35.

To generate a more detailed description of the central region of the site, a new cluster was calculated from the surface points within 6 Å of the center of mass of the site. Spheres with centers farther than 5 Å from the center were eliminated. CLUSTER, a program that tailors the sphere sets (Shoichet et al., 1992), was then run on the remaining spheres to give a final cluster composed of 27 spheres. Parameters input to CLUSTER are listed in Table I, column II. More detailed DOCK2 runs used this cluster and the parameters listed in Table I, column VI. A higher resolution scoring grid calculated with the parameters in Table I, column V, used close contact limits more representative of the distances observed in the crystallographic complex of an inhibitor bound to a hydrophobic pocket (Badger et al., 1989). Docking 5000 compounds to the 27-sphere cluster required 30 h of cpu time on an IRIS 4D/35.

Hardware, Software, and *Databases.* Molecular surfaces were computed with DMS (C. Huang, personal communication), a distributed processing implementation of Connolly's MS algorithm (Connolly, 1983). Protein sites, small molecules, and their surfaces were displayed with MIDASPLUS (Ferrin et al., 1988). MACCS-II/3D (Revision 1.0) and the Fine Chemicals Directory database (FCD3D_89.2) were provided by Molecular Design, Ltd. (San Leandro, CA). SPHGEN, CLUSTER, DISTMAP, and DOCK2 are available from the authors. MACCS and SPHGEN were run on a VAX 8650, and DMS was run on SUN SPARCstations (SUN Microsystems, Inc., Mountain View, CA). All other computation and graphics visualizations were done on an IRIS 4D/35 (Silicon Graphics, Mountain View, CA).

RESULTS

Target Site Selection. Since none of the previously studied sites on HA are known to regulate fusion peptide exposure, a site that could have this activity had to be discovered. Typically, novel sites are identified with DOCK by analyzing all invaginations on a receptor surface. However, the large size of HA made it computationally infeasible to examine the entire ectodomain. Instead, only sites in the vicinity of the fusion peptide were initially considered since they seemed most likely to affect fusion peptide exposure.

The site selected for targeting an inhibitor should also have features conducive to ligand binding. Since binding affinity is predominantly determined by hydrophobic interactions (Fersht, 1984), surfaces proposed to interact directly with a ligand should include contributions from hydrophobic residues. The site should also possess charged residues that can be exploited for designing specificity into a ligand and should be solvent accessible and free of carbohydrate residues.[2]

Of all the concave regions identified in the vicinity of the fusion peptide, one site fit the chemical criteria particularly well. This site is defined by residues of a single monomer but

[2] Density for most of the carbohydrate chains is not visible in the electron density maps of BHA, so the possibility of a site being filled by sugar moieties was estimated by its proximity to glycosylated residues 8, 22, 38, 81, 165, and 285 of HA1 and 154 of HA2.

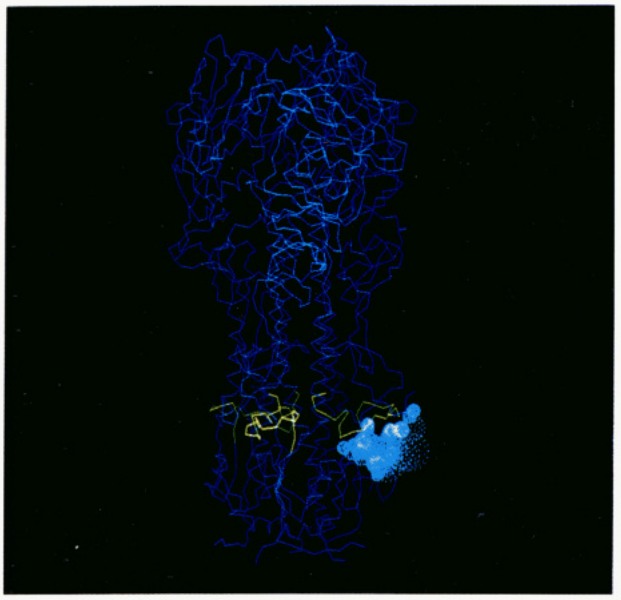

FIGURE 1: Location of the target site on the BHA trimer. Spheres defining the site (cyan) are superimposed on the α-carbon backbone of the trimer (dark blue). Identical sites exist in each monomer of the trimer. The three fusion peptides are colored yellow.

lies near the interface with a second monomer. The location of the site on the trimer is shown in Figure 1. The site is solvent accessible, no carbohydrate atoms present in the PDB file lie within 20 Å of the site, and the nearest glycosylated residue, Asn 154 of HA2, is 25 Å away from the center of the site on the other side of the trimer. Not only is the site in the vicinity of the fusion peptide, its medial region is defined by fusion peptide residues 4, 7–19, and 24 of HA2 (Figure 2a). The pocket is approximately 10 Å wide and 10 Å deep[3] and has a bowl-like shape. At the base of the bowl is a dimple-like extension lying over His 17 of HA1. Side chains of hydrophobic residues contribute 112 Å^2 of the surface in the center of the site (Figure 2b). Small molecules specific for this particular site can be designed to complement the charges on residues Glu 325 of HA1 and Glu 11 and Arg 25 of HA2 lining the rim of the site and His 17 of HA1 in the dimple[4] (Figure 2b). Comparison of the residues comprising the site revealed it to be highly conserved among hemagglutinins from a wide variety of strains of influenza (Table II) (Bodian, 1992).

Selection of Candidate Ligands. Compounds that might bind to the target site were identified by searching the Fine Chemicals Directory (FCD) for small molecules with steric and electrostatic complementarity to the intended binding site. An initial search was done at low resolution (see Materials and Methods). High scoring compounds were screened graphically to identify classes of structures with appropriate shape or which positioned substituents near one or more of the charged groups surrounding the site. Members of the selected chemical classes were then redocked at higher resolution. Of the ~55 000 small molecules present in the complete database, 5000 were selected for the higher resolution analysis. Several hundred of the ligands receiving high scores in the second docking were then examined graphically for those predicted to interact with residues of the fusion peptide, charged residues of the site, and/or hydrogen bond donors or acceptors within the site. The best compounds were also structurally rigid, chemically stable, easily desolvated, water-soluble, and commercially available. Of the 5000 compounds, 48 were selected for experimental screening. Representative structures illustrating the variety of chemicals selected are shown in Figure 3.

Inhibition of Fusion Peptide Exposure. The selected compounds were screened for their ability to inhibit fusion peptide exposure by a scintillation proximity assay [see Bosworth and Towers (1989)]. This assay is similar to immunoprecipitation in that it detects protein specifically recognized by a primary antibody such as an α-fusion peptide antibody. However, in the SPA, the primary antibody–protein complexes are detected by binding to SPA beads, microspheres coupled to both scintillant and protein A. To test for inhibition, purified [^{3}H]BHA was preincubated with or without test ligands and then exposed to low pH. Following reneutralization, the protein was incubated with fusion peptide antiserum and SPA beads. Since the fusion peptide antibody only reacts with HA that had undergone the conformational change (White & Wilson, 1987), inhibition of fusion peptide exposure is evidenced by a reduction in the number of cpm detected compared to otherwise identical samples with the trial compound omitted.

However, inhibition of the conformational change by binding to HA is not the only way in which the compounds could reduce the detected cpm. (1) The compounds could prevent fusion peptide exposure by altering the pH of the low pH solution. To eliminate this possibility, the pH of a solution of any compound showing apparent inhibition was measured. (2) The compounds could prevent the detection of fusion peptide antibody–low pH BHA complexes. For example, the compounds could prevent binding between the antibody and the SPA beads, or they could quench the signal emitted by the scintillant. "POST" control samples distinguished whether any observed reduction in cpm was due to inhibition of the conformational change or to nonspecific effects. A sample of BHA was acidified in the absence of test compounds to convert it to the low pH conformation. The trial compound was added immediately after reneutralization but prior to incubation with antibody and SPA beads. Any observed reduction in cpm in these samples indicated some interference with the detection system.

The commercial compounds selected from the FCD were screened by SPA using the α-fusion peptide antibody. Highly toxic compounds or compounds insoluble in DMSO or water were not tested. Compounds were screened at 10^{-3} M, or, for those insoluble at 1 mM, in a saturated solution. POST controls were run for all compounds which reduced the cpm by at least 10%. Of 43 ligands tested, only one, compound 83 (structure shown in Figure 10 as 83K), reproducibly reduced the number of counts detected, did not reduce the number of cpm in the POST control, and did not alter the pH of the low pH solution. The dose response curve in Figure 4 shows that this compound exhibited half-maximal inhibition at approximately 5×10^{-4} M.

Inhibition Is Reversible by Dilution. The inhibition observed with compound 83 is presumably due to an interaction with hemagglutinin. A dilution experiment was conducted to distinguish whether the interaction is noncovalent or covalent. If inhibiton is due to noncovalent binding, it should be reversible by dilution. Compound 83 was incubated with BHA at an initial concentration of 10^{-3} M. Half of the mixture was then diluted to 10^{-5} M, a concentration at which negligible inhibition had been observed (Figure 4). The other half was diluted to the same volume, but the concentration of compound 83 was

[3] Atom NH1 of Arg 25 (HA2) is 10.23 Å from atom OE2 of Glu 25 (HA2) and 11.0 Å from atom ND1 of His 17 of HA1.

[4] The charged states of His 17 and His 18 of HA1 at neutral and endosomal pHs are unknown.

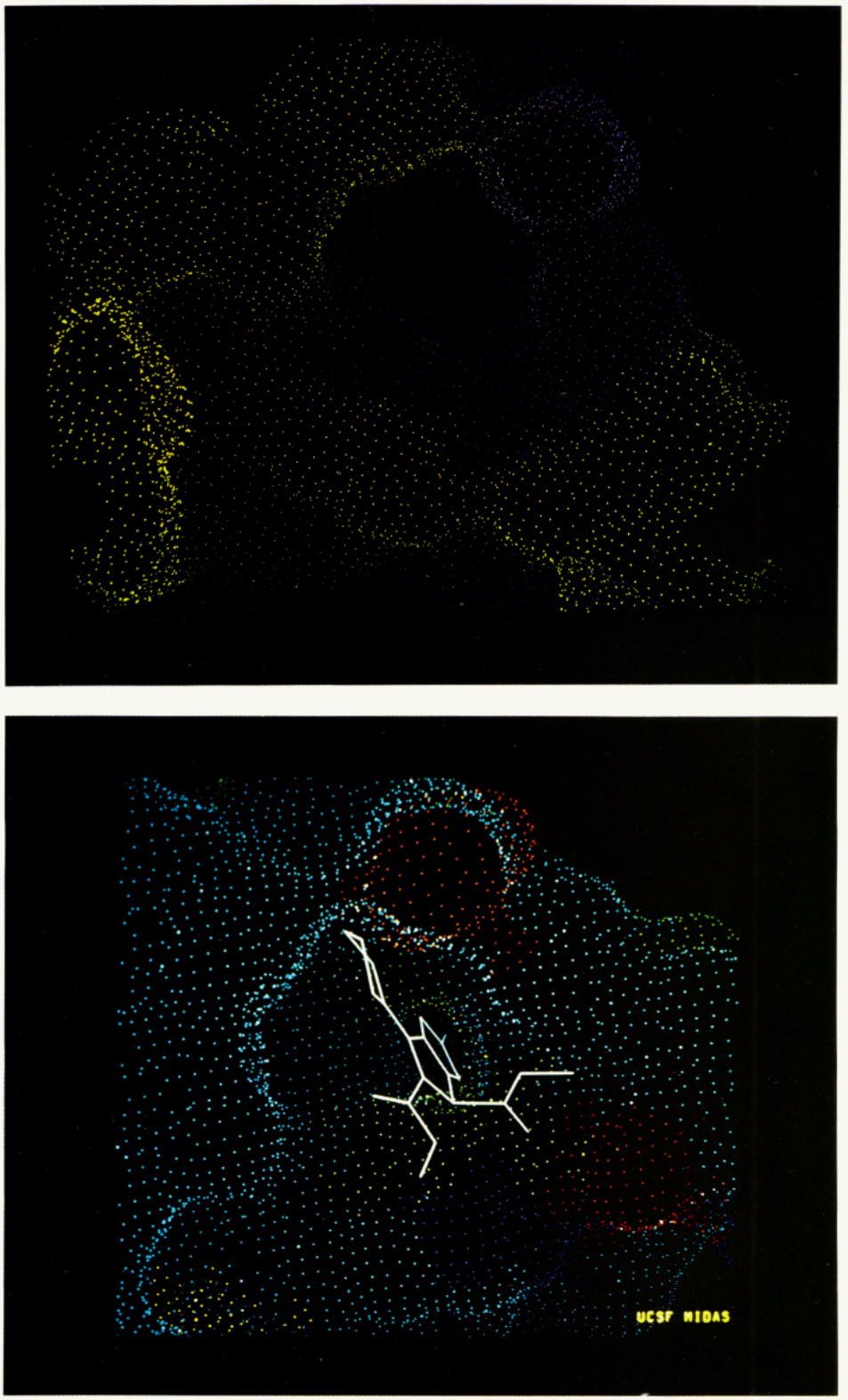

FIGURE 2: (a, top) Surface of the target site contributed by residues of the fusion peptide. Molecular surface points derived from residues 4–19 of HA2 are shown in magenta. (b, bottom) The target site colored by chemical functionality. Red represents the surface contributed by carboxylic acid moieties of glutamate and aspartate, blue represents the guanidinium of arginine and the amine of lysine. Histidine side chains are colored yellow. Surface points contributed by hydrophobic side chains are shown in green. The displayed compound (white) is for illustration only.

maintained at 10^{-3} M. Acidification and SPA reactions were carried out as usual. The results in Table III reveal that the inhibition caused by compound 83 at 1 mM was reversible by dilution, suggesting that the interaction with BHA is noncovalent.

Inhibition as a Function of Time at Low pH. To characterize further the effect of compound 83, inhibition was measured as a function of time at low pH. If the activity of 83 is due to chemical reactivity of the compound at pH 5, inhibition should remain constant or increase during extended incubations at low pH. If the effect is noncovalent, then, due to the irreversibility of the conformational change itself, inhibition would be expected to decrease as a function of time. The results through 10 min of exposure to pH 5.0 are shown

Table II: Conservation of Residues Defining the Target Site[a]

sequences	no. of sequences HA1/HA2[b]	% identity target site	% identity complete HA
human H3	19/11	99.5	96.3
all H3	40/32	96.7	94.4
all	85/70	81.9	73.6

[a] The 60 residues defining the site (11–21, 320, and 323–328 of HA1 and 4–19, 21–28, 31–35, 115, 119, 121, 124–125, 132–138, and 149 of HA2) were compared among hemagglutinins from all sequenced strains of influenza A including H1, H2, H3, H4, H5, H6, H7, H8, H9, H10, H11, and H12 subtypes isolated from mammals and birds (Bodian, 1992). [b] Sequence data for several strains are only available for the less highly conserved HA1 polypeptide.

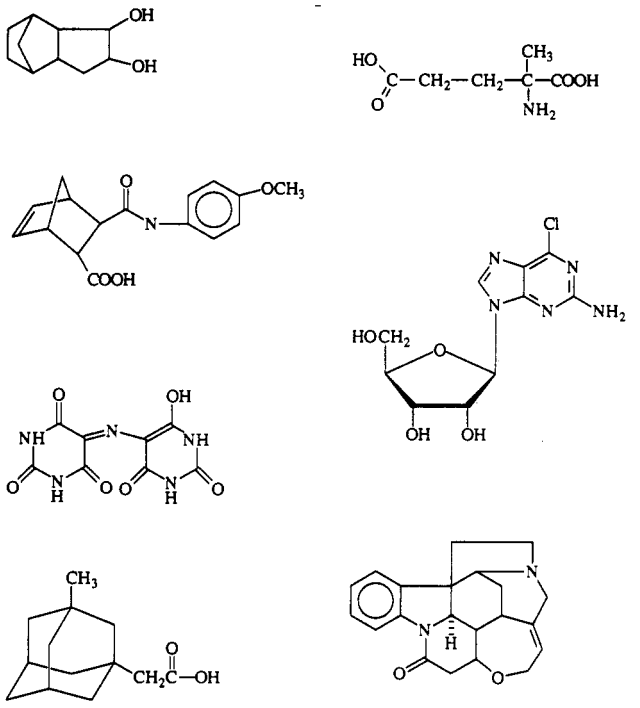

FIGURE 3: Sample of the variety of structures selected for screening.

in Figure 5. Initially, at 10 s, 73% inhibition was observed. After 10 min, inhibition had decreased to 43%. This implies that inhibition is reversible at low pH. The plateauing of the curve is presumably caused by the decreased ability of HA to be recognized by the fusion peptide antibody after extended exposure to low pH (Puri et al., 1990; J. White, unpublished results). Combined with the results of the dilution experiment, the data suggest that compound 83 is a reversible inhibitor.

Inhibition by Isomers of 83. The commercially available compound 83 may be a mixture of tautomers. The two isomers, 83K and 83A (structures shown in Figure 10), were prepared separately and tested individually (Figure 6). The concentration profile of 83K exactly mimics that of the commercially available 83, but compound 83A was active at 100-fold lower concentrations. Although this suggests that both compounds can inhibit fusion peptide exposure, it is formally possible that the inhibition observed with 83 and 83K is due to a 1% contamination by 83A, possibly generated during the course of the experiment.

Selection and Activity of Derivatives of 83K and 83A. The substructure searching facility of MACCS-II/3D was used to find compounds chemically related to 83K and 83A. Approximately 50 derivatives were selected and then screened by SPA. Table IV lists the IC_{50}s of representative compounds (structures shown in Figure 10). The derivatives inhibited fusion peptide exposure with activities ranging from inactive

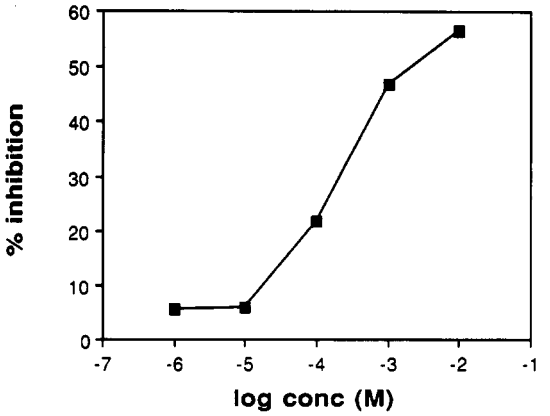

FIGURE 4: Dose–response of compound 83 in the SPA. Percent inhibition is averaged over duplicate precipitations from 1–3 independent experiments. The millimolar point is the average of 16 independent determinations. Values are corrected for nonspecific quenching as described under Materials and Methods. Inhibition of the POST controls was 26.4% at 10 mM and 4% or less at all other concentrations. Standard deviations are as follows: 1 μM, 9.5; 10 μM, 19.6; 0.1 mM, 17.1; 1 mM, 15.0. These errors reflect the daily variability of the activity at each concentration. Standard deviation from duplicate samples within a single experiment are approximately 3%.

Table III: SPA Dilution Experiment with Compound 83

sample[a]	conc (M)	% inhibition[b]
1	$10^{-3} \rightarrow 10^{-3}$	45.3
2	$10^{-3} \rightarrow 10^{-5}$	4.6

[a] Samples were preincubated with 1 mM 83. Sample 1 was maintained at 10^{-3} M throughout the experiment, but sample 2 was diluted to 10^{-5} M prior to acidification. All samples were incubated at low pH for 5 min and then subjected to SPA with the α-fusion peptide antibody. [b] Percent reduction in cpm compared to controls with 83 omitted. POST controls showed no nonspecific quenching by 83 at these concentrations.

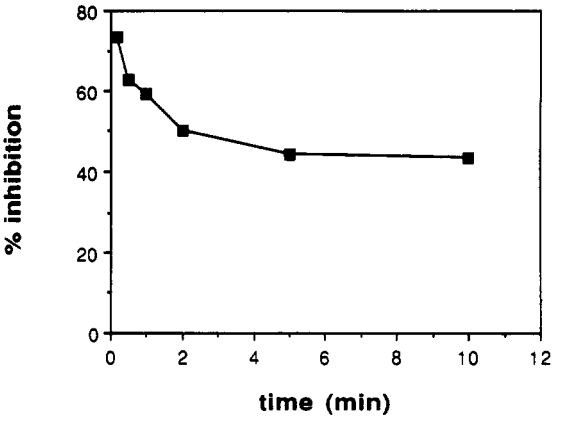

FIGURE 5: Inhibition by compound 83 as a function of time at low pH. The cpm detected by SPA in the presence of 1 mM 83 were compared to those in samples without 83.

at millimolar concentrations to inhibitory in the micromolar range. Control experiments revealed that none of the compounds tested affected the pH of the reactions.

Effect of Compounds on Hemagglutination. Compounds inhibiting fusion peptide exposure were tested for their ability to inhibit fusion and infectivity. Assays measuring these processes depend on viral recognition of cellular receptors. To rule out the possibility that any observed inhibition in these experiments was due to inhibition of virus–cell binding, hemagglutination tests were performed. None of the compounds tested, including 83 (1 mM), 91 (1 mM), and 117 (10 μM), prevented binding between intact virions and their receptors on red blood cell membranes (data not shown).

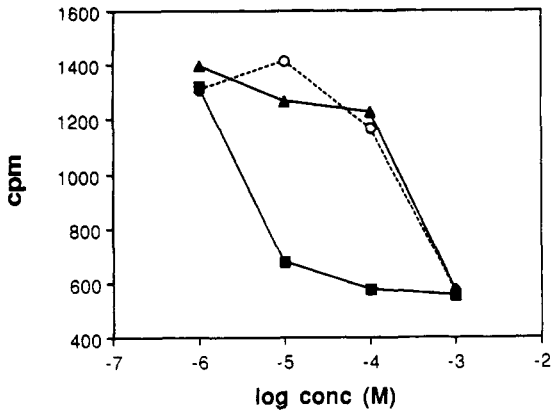

FIGURE 6: Effect of compounds 83 (○), 83K (▲), and 83A (■) on SPA. The cpm are averaged from duplicate samples from a single experiment.

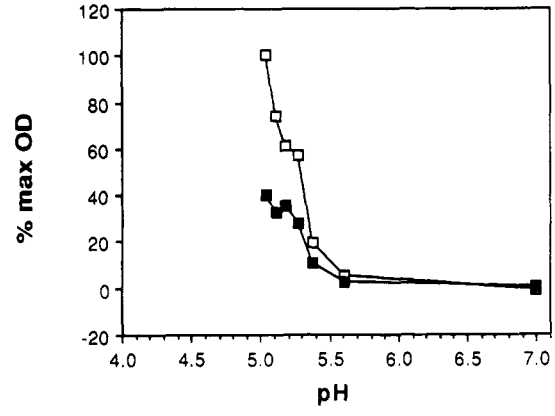

FIGURE 7: Hemolysis with compound 91 as a function of pH. (■) Samples containing 0.1 mM 91; (□) samples without 91. The OD_{570}'s of control samples at pH 5.0 and 7.0 were taken as 100% and 0%, respectively. Inhibition was not measured below pH 5.0 since hemolysis in control samples at lower pHs is reduced by an unknown mechanism (Bodian, 1992; Maeda et al., 1981).

Effect on Fusion: Hemolysis. The ability of the compounds to inhibit fusion was first tested by a hemolysis assay. Influenza viruses rupture the membranes of red blood cells under fusion-inducing conditions. The amount of hemoglobin released, as measured by the absorbance at 570 nm, is proportional to the amount of fusion. Therefore, compounds capable of preventing hemagglutinin-mediated fusion should reduce the OD by an amount related to the inhibitory activity.

Two sets of controls detected compound-induced effects on red blood cells. (1) Samples containing compounds but not virus measured whether any compound lysed red blood cells in the absence of virus. (2) Control samples containing hemoglobin instead of intact red blood cells determined if the compounds affected the OD_{570} by altering the absorption spectrum of hemoglobin. None of the compounds had significant absorption at OD_{570} themselves at the concentrations tested.

The hemolysis results corrected for the nonspecific effects described above are shown in Table IV. Compounds 83, 90, 91, 111, and 117 apparently inhibited hemolytic activity. The effect of 107 on virus-induced hemolysis could not be measured due to a complete loss of OD_{570}. All compounds that inhibited hemolysis also inhibited fusion peptide exposure, while compounds not showing inhibition of hemolysis did not inhibit the SPA. These data suggest that certain derivatives of 83 are able to inhibit hemagglutinin-mediated hemolysis.

Figure 7 shows virus-induced hemolysis with compound 91 at 0.1 mM as a function of pH. Maximum inhibition (61.0%) was observed at pH 5.0. Figure 7 also reveals that compound 91 shifts the pH profile of hemolysis by approximately –0.2 pH units.

Effect on Fusion: Fluorescence Dequenching. The ability of the compounds to inhibit fusion was also tested in a fluorescence dequenching (FDQ) experiment. FDQ is a function of the baseline fluorescence at neutral pH, the fluorescence as a function of time at low pH, and the fluorescence at infinite probe dilution, approximated in a detergent solution. Several of the compounds quenched each of these measurements by unequal amounts and thus prevented reliable determination of inhbition of lipid mixing. Inhibition could also not be measured for compounds such as 114 which are either fluorescent themselves or relieved self-quenching of the fluorescent probe by a fusion-independent mechanism. Compounds which did not exhibit these problems, including 99 (10 or 100 mM) and 116 (1 or 0.1 mM), did not inhibit HA-mediated FDQ at the concentrations tested. These latter data are in agreement with the SPA and hemolysis data (Table IV) suggesting that, at these concentrations, compounds 99 and 116 do not inhibit fusion.

Effect on Fusion: Syncytia Formation. The ability of the compounds to inhibit virus-induced cell–cell fusion was measured by a syncytia assay. Compounds that prevent fusion will inhibit formation of polykaryons. Only nontoxic compounds which did not visibly affect the morphology of the cells were screened by this assay. To be in the linear range of the experiment, the amount of virus used was only enough to induce fusion of ~50% of the cells. As shown in Figure 8, 117 at 10^{-5} M almost entirely inhibited syncytia formation. Dilution of 117 to 10^{-6} M greatly reduced the extent of inhibition. In contrast, no inhibition was observed with compound 120 at 10^{-5} M. These results with both 117 and 120 are consistent with the results of SPA and hemolysis with these compounds (Table IV). Cell–cell fusion mediated by the HIV-1 fusion protein was not inhibited by 117 at 10 μM (C. Weiss, personal communication), suggesting that 117 is not a general fusion inhibitor.

Inhibition of Infectivity. To determine whether the compounds which inhibit fusion peptide exposure, hemolysis, and syncytia formation can also inhibit viral replication, the ability of the compounds to prevent influenza infectivity was measured by a single-cycle infectivity assay. Viability assays were conducted in parallel to test whether any observed inhibition of infectivity could be accounted for by cell death. While some of the compounds were toxic at the concentrations tested, others were able to inhibit viral replication under conditions at which the cells were viable. The concentration profiles of one compound, 117, in the infectivity and viability assays are compared in Figure 9. The data for selected compounds listed in Table IV show that the concentrations effective in preventing infectivity are similar to those effective in the SPA and syncytia assays.

DISCUSSION

A crucial early stage of virus replication is fusion between the viral membrane and a membrane of the host cell. This step is potentially susceptible to intervention by antiviral agents. Fusion is dependent on conformational changes of the viral fusion protein. Influenza HA is the best characterized fusion protein and has served as a model for the fusion proteins of other viruses (Stegmann et al., 1989; White, 1990; Wiley & Skehel, 1987). Development of inhibitors of the conformational change of HA could not only lead to novel anti-influenza drugs but also illustrates a strategy potentially applicable to inhibition of enveloped viruses in general.

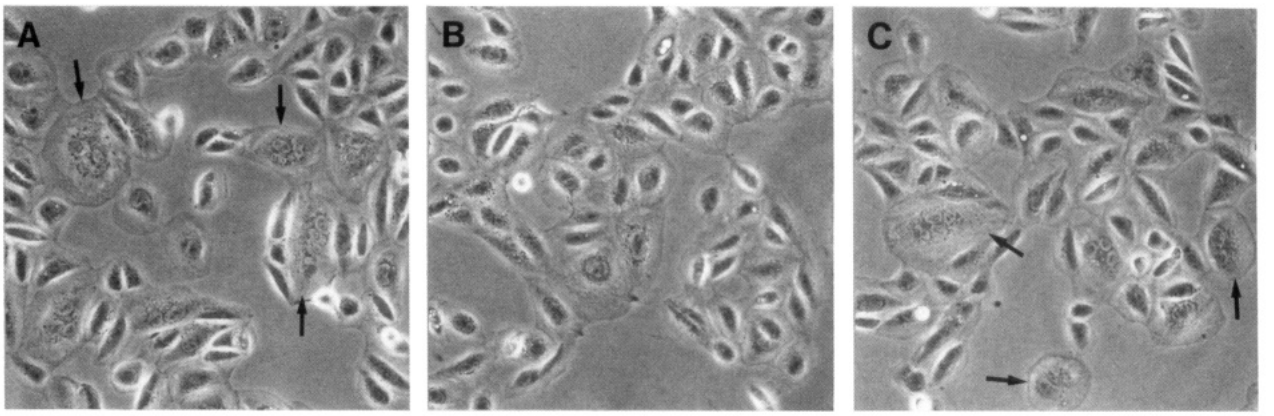

FIGURE 8: Effects of selected compounds on influenza-induced syncytia formation. Wells were incubated with (A) DMSO, (B) 10 μM 117, and (C) 10 μM 120. Arrows indicate examples of syncytia.

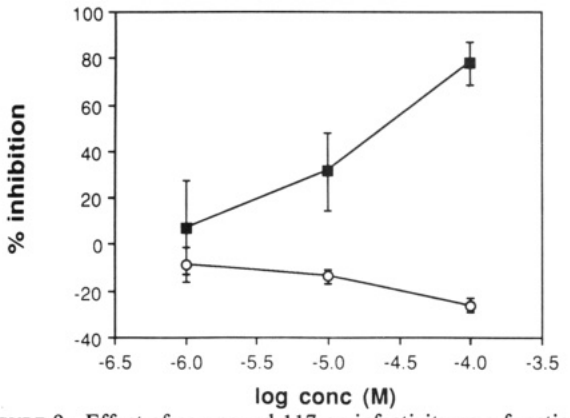

FIGURE 9: Effect of compound 117 on infectivity as a function of concentration. (■) Inhibition of single cycle infectivity. (○) Inhibition of cell viability.

Mechanism of Inhibition. We have identified compounds which inhibit fusion peptide exposure of HA and prevent hemolysis, syncytia formation, and infection by X31 influenza viruses. At least part of the inhibition detected in the four independent assays is likely to result from a common mechanism. Among the inhibitory compounds, there is good agreement between the concentration profiles observed in the fusion peptide exposure (SPA), syncytia, and infectivity assays (summarized in Table IV). Moreover, compounds which did not inhibit fusion peptide exposure also did not inhibit hemolysis, syncytia formation, or infectivity at levels unaccounted for by nonspecific effects[5] (Table IV and data not shown). The target of the inhibitory compounds must therefore be the fusion-inducing conformational change, the only step shared by all the experiments. The ability of compound 83 to inhibit fusion peptide exposure even after 10 min at pH 5 (Figure 5) is consistent with the idea that the compounds could inhibit the conformational change along the cellular endocytic pathway long enough to prevent infectivity.[6]

The mechanism by which the compounds inhibit the conformational change is apparently noncovalent. Inhibition was relieved by dilution (Table III) or by extended lengths of exposure to low pH (Figure 5). The compounds presumably interact specifically with HA and not proteins in general since they do not abolish the binding capacity of fusion peptide antibodies, protein A, or the hemagglutinin receptor(s) on red blood cells.

The inhibitory compounds may be partial antagonists of fusion peptide exposure. Averaged over five independent SPA experiments, the maximum observed inhibition with all nonquenching compounds was 65.6 ± 7.8%. This maximum could not be increased by raising the concentration of ligand (data not shown) or by extending the incubation of the compounds with hemagglutinin up to 4 h (data not shown). Since the BHA used in the experiments was >90% pure and no cpm were detected without prior acidification, the residual 34% cannot be attributed to a radiolabeled contaminant. One explanation for incomplete inhibition is that a fraction of the BHA trimers is misfolded or otherwise uninhibitable. A second possibility consistent with the data is that the compounds are unable to inhibit the conformational change of native trimers completely. Previous work has demonstrated that the conformational change of the trimer depends on the ability of each monomer to change conformation (Boulay et al., 1988). Therefore, complete inhibition may require inhibition of conformational changes in every monomer. If the compounds cannot prevent fusion peptide exposure on all three monomers simultaneously, it is likely that partial inhibition would result.

A second observation bearing on the fusion mechanism of HA is that higher concentrations of inhibitors were required for 50% inhibition of hemolysis than to achieve comparable levels of inhibition of syncytia formation, infectivity, or fusion peptide exposure (Table IV). This suggests that the extent of conformational changes required for hemolysis differs from that necessary for syncytia formation and infectivity. A similar conclusion is suggested by studies of mutant hemagglutinins which were able to mediate red blood cell fusion under conditions at which syncytia formation was not observed (Gething et al., 1986).

Site of Inhibition. At this time, we do not know the binding site(s) of the inhibitory compounds. We only know that they have the capacity to affect conformational changes in the stem of HA. The binding site may be the targeted site adjacent to the fusion peptide or a site elsewhere on the trimer. Modeling experiments showed that the compounds can fit other sites besides the targeted site equally well, notably a site in the hinge region of HA (Bodian, 1992). Experimental determination of the site of action of the compounds could have interesting implications for the mechanism of the conformational change. If the compound binds to a site(s) distant from the fusion peptide, it would support the conclusion

[5] Compound 116, inactive in the SPA and hemolysis but modestly inhibitory in infectivity, presumably prevented viral replication by a mechanism other than inhibition of the conformational change of HA.

[6] The antiviral compound does not necessarily have to prevent conformational changes along the entire endocytic pathway. It is possible that hemagglutinin reaching a pre-lysosomal compartment with a pH below the fusion threshold will undergo rearrangements that inactivate its fusion potential.

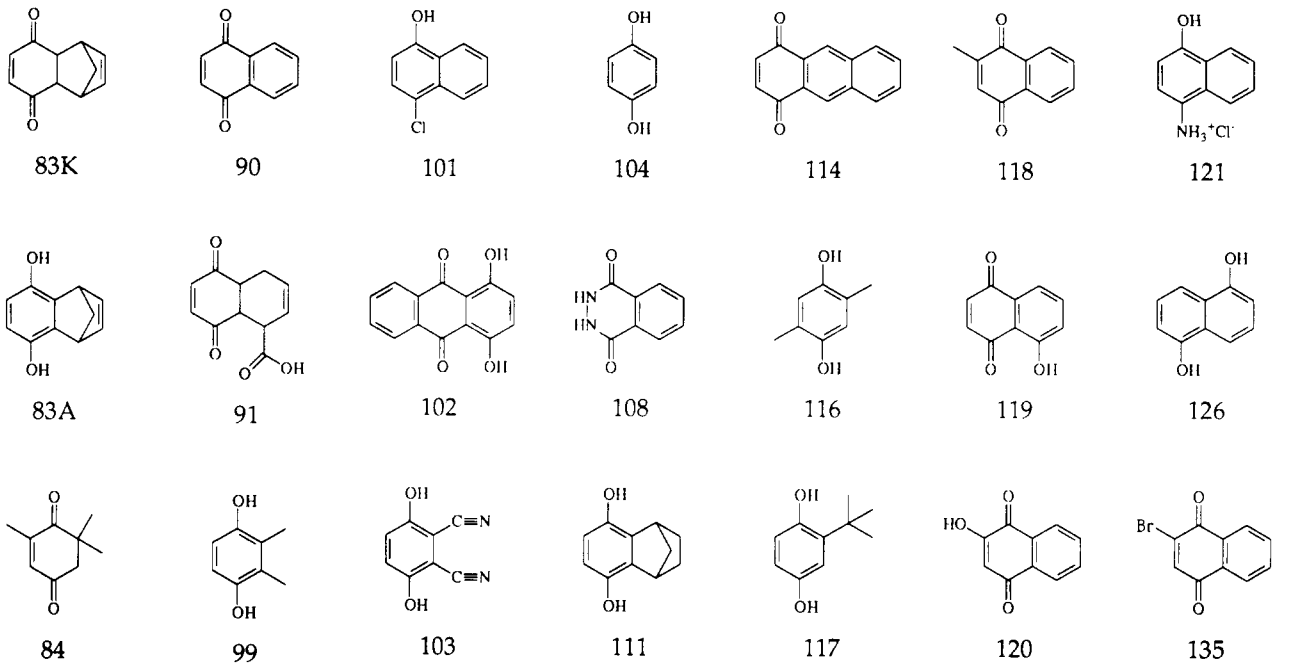

FIGURE 10: Structures of 83A, 83K, and the derivatives listed in Table IV.

Table IV: Compound Activities in the Scintillation Proximity, Hemolysis, Syncytia, Infectivity, and Viability Assays

	IC_{50} (μM)[a]				CC_{50} (μM)[a]
compound	SPA[b]	hemolysis[b]	syncytia	infectivity[c]	toxicity[d]
99	>1000	>1000	toxic[g]	15	60
101	>1000	quench[f]	nd	nd	>100
102	>1000	nd	nd	nd	nd
103	>1000	>1000	nd	nd	nd
104	>1000	nd	nd	nd	nd
108	>1000	nd	nd	nd	nd
116	>1000	>1000	morph[h]	15	>100
118	>1000	nd	nd	nd	30
120	>1000	>100	>10	>100	>100
121	>1000	>1000	nd	nd	10
135	>1000	>1000	nd	nd	nd
119	>100	nd	nd	nd	30
84	1000	nd	nd	nd	>100
126	1000	1000	nd	>100	>100
83K	250	500	nd	nd	100
90	200	1000	morph[h]	4	>10
83A	25	–[i]	nd	–[i]	–[i]
91	10	100	nd	25	>100
111	10	500	morph[h]	6	>100
114	8	nd	toxic[g]	3	8
117	5	100	6[e]	20	>100

[a] Calculation of the concentrations at which 50% inhibition was observed is described under Materials and Methods. Only 10-fold dilutions were tested except that 117 was tested in the syncytia assay at 1, 3, and 10 μM. All data are averaged from every replication of each experiment. [b] The IC_{50} has been corrected for nonspecific inhibition as described under Materials and Methods. [c] Data from independent replications of the infectivity experiment suggest that the listed values are accurate within 0.4 log units, or a factor of 2.5. [d] Viability data are accurate within 0.07 log units (1.2). [e] The IC_{50} for 117 in syncytia lies between 3 and 10. [f] Inhibitory activity could not be assessed due to quenching by the compound. [g] The compound was toxic to the cells at the tested concentrations. [h] morph, the compound altered the morphology of the cells. [i] Compound 83A was initially inhibitory in the SPA assay but lost activity as it aged. No active sample was available for texting in the other assays. nd, not done.

from recent studies that the conformational change is cooperative throughout much of the trimer (Godley et al., 1992; Kemble et al., 1992).

The site identified by the modeling may prove useful for future inhibitor design efforts. Even if it is not the actual binding site of the compounds reported here, it is still an attractive site for targeting potential inhibitors of the conformational change. The high conservation of the site among known strains of influenza (Table II) and its proximity to the fusion peptide (Figures 1 and 2a) suggest that the site has an important role in the functioning of hemagglutinin. The high conservation also predicts that a compound which inhibits X31 hemagglutinin by binding to the site could also inhibit hemagglutinins from a wide range of strains. Further support for the importance of the site comes from studies of mutant hemagglutinins with substitutions in residues composing the site. HAs with mutations at position 17 of HA1, located at the base of the target site, fuse at elevated pH (Daniels et al., 1985; Rott et al., 1984). While it is unknown whether the mutations alter hydrogen-bonding patterns, site geometry, and/or the electrostatic environment, they show that residues of the target site can affect fusion peptide exposure.

Implications for Drug Design. Independent of their mechanism of inhibition, the compounds do possess antiviral activity in vitro. While they are not expected to be useful therapeutic agents themselves, they could lead to the discovery of more effective analogs. Such derivatives will be based on a model summarizing the functional groups observed to increase or decrease inhibition (see, for example, Figure 11). High-resolution structural information from complexes of inhibitory compounds and BHA could also suggest features, perhaps based on alternate chemical frameworks, likely to improve binding. Any compound with sufficiently high affinity will be tested for its pharmacologic properties and its ability to inhibit other strains of influenza.

Identification of inhibitors of the conformational change was a particularly stringent test of rational inhibitor design. Rational design methods are typically used to identify inhibitors of an enzymatic activity. Unlike targeting an enzyme active site, discovery of an inhibitor of a conformational change requires identification of a novel binding site that could effect the desired activity as well as selection of trial compounds with no knowledge of chemical groups likely to determine binding to the site. To date, rational design of de novo inhibitors of any conformational change has only produced inhibitors of the transition between the oxy- and deoxy- forms

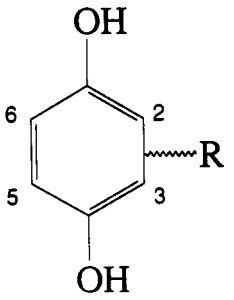

FIGURE 11: Summary of the structural features shared among inhibitory compounds. "R" represents a single hydrophobic ring fused at the 2–3 bond or a hydrophobic substituent smaller than a phenyl ring at the 2 position. The strongest inhibitors were 1,4-hydroquinones with a hydrophobic ring system fused at the 2–3 bond or a hydrophobic substituent smaller than a phenyl ring at the 2 position. Analogous benzoquinones were also active. Derivatives substituted at both C2 and C3 (other than a fused ring) or at C6 showed weaker inhibition.

of hemoglobin (Beddell et al., 1976, 1984). However, a cocrystal with one of these compounds showed that while it binds to the targeted site, it does so in an orientation differing from the prediction (Wireko & Abraham, 1991). Although proof that the anti-influenza compounds described here bind to the targeted site on HA awaits determination of a high-resolution structure, the inhibitor design method did identify novel inhibitors with the desired activity. The lead compound was discovered after testing only 43 compounds, compared to the thousands typically evaluated in random screening trials (Korolkovas & Burckhalter, 1976). Use of a database of commercially available compounds was undoubtedly invaluable in contributing to the success since it enabled easy acquisition of a wide variety of structures for testing.

Extension to Other Viruses. The data presented here and studies with norakin, an inhibitor of fowl plague virus, an avian influenza virus (Ghendon et al., 1986; Presber et al., 1984), and with a mutant X31 HA (Godley et al., 1992; Kemble et al., 1992) suggest that inhibition of the conformational change of a viral fusion protein can prevent fusion and infectivity. Inhibition of fusion has been largely unexplored as a target for antiviral development (Hirsch & Kaplan, 1990) and has the advantage of interfering with an early step in replication. As it does not aim to inhibit an enzymatic activity or to mimic any natural ligands the chance of fortuitous inhibition of unintentional targets is minimized. Since fusion is a step common to the replication of all enveloped viruses, this antiviral strategy can potentially be applied to a large number of other viral diseases including rubella, mumps, measles, rabies, and herpes.

Other inhibitors that interact with viral proteins and block fusion or penetration have been discovered but only serendipitously (Caliguiri et al., 1980; Gruenberger et al., 1991; McSharry et al., 1979; Otto et al., 1985; Schroeder et al., 1985). The compounds reported here represent the first antiviral agents intentionally designed to inhibit the protein conformational changes required for entry. As three-dimensional coordinates of other fusion proteins become available from biophysical experiments or from modeling, fusion inhibitors can be designed against an increasing number of enveloped viruses.

ACKNOWLEDGMENT

We thank Lilia Babé, Brian Shoichet, Elaine Meng, Patricia Caldera, and Joe Nugent for helpful discussions and for their experimental and computational contributions. Anne Bartfay and Manjita Bhaumik provided technical assistance. We thank the Influenza Group at the Centers for Disease Control in Atlanta for help with virus preparation and for the EIA protocol. This work was done in part with the facilities of the UCSF Computer Graphics Laboratory.

REFERENCES

Abola, E. E., Bernstein, F. C., Bryant, S. H., Koetzle, T. F., & Weng, J. (1987) in *Crystallographic Databases—Information Content, Software Systems, Scientific Applications* (Allen, F. H., Bergerhoff, G., & Seivers, R., Eds.) pp 107–132, Data Commission of the International Union of Crystallography, Cambridge.

Badger, J., Minor, I., Oliveira, M., Smith, T., & Rossmann, M. (1989) *Proteins 9*, 1–19.

Beddell, C. R., Goodford, P. J., Norrington, F. E., Wilkinson, S., & Wootton, R. (1976) *Br. J. Pharmacol. 57*, 201–209.

Beddell, C. R., Goodford, P. J., Kneen, G., White, R. D., Wilkinson, S., & Wootton, R. (1984) *Br. J. Pharmacol. 82*, 397–407.

Bernstein, F. C., Koetzle, T. F., Williams, G. J. B., Meyer, E. F., Jr., Brice, M. D., Rodgers, J. R., Kennard, O., Shimanouchi, T., & Tasumi, M. (1977) *J. Mol. Biol. 112*, 535–542.

Bodian, D. L. (1992) Ph.D. Thesis, University of California, San Francisco.

Bosworth, N., & Towers, P. (1989) *Nature 341*, 167–168.

Boulay, F., Doms, R. W., Webster, R. G., & Helenius, A. (1988) *J. Cell Biol. 106*, 629–639.

Caliguiri, L. A., McSharry, J. J., & Lawrence, G. W. (1980) *Virology 105*, 86–93.

Connolly, M. L. (1983) *Science 221*, 709–713.

Daniels, R. S., Downie, J. C., Hay, A. J., Knossow, M., Skehel, J. J., Wang, M. L., & Wiley, D. C. (1985) *Cell 40*, 431–439.

DesJarlais, R. L., Sheridan, R. P., Seibel, G. L., Dixon, J. S., Kuntz, I. D., & Venkataraghavan, R. (1988) *J. Med. Chem. 31*, 722–729.

Doms, R. W., Helenius, A., & White, J. (1985) *J. Biol. Chem. 260*, 2973–2981.

Doms, R. W., Gething, M.-J., Henneberry, J., White, J., & Helenius A. (1986) *J. Virol. 57*, 603–613.

Ferrin, T. E., Huang, C. C., Jarvis, L. E., & Langridge, R. (1988) *J. Mol. Graphics 6*, 13–27.

Fersht, A. R. (1984) *Trends Biochem. Sci. 9*, 145–147.

Gething, M.-J., Doms, R. W., York, D., & White, J. (1986) *J. Cell Biol. 102*, 11–23.

Ghendon, Y., Markushin, S., Heider, H., Melnikiv, S., & Lotte, V. (1986) *J. Gen. Virol. 67*, 1115–1122.

Godley, L., Pfeifer, J., Steinhauer, D., Ely, B., Shaw, G., Kaufmann, R., Suchanek, E., Pabo, C., Skehel, J. J., Wiley, D. C., & Wharton, S. (1992) *Cell 68*, 635–645.

Gruenberger, M., Pevear, D., Diana, G. D., Kuechler, E., & Blaas, D. (1991) *J. Gen. Virol. 72*, 431–433.

Grunwell, J. R., Karipides, A., Wigal, C. T., Heinzman, S. S., Parlow, J., Surso, J. A., Clayton, L., Fleitz, F. J., Daffner, M., & Stevens, J. E. (1991) *J. Org. Chem. 56*, 91–95.

Hirsch, M. S., & Kaplan, J. C. (1990) in *Virology* (Fields, B. N., & Knipe, D. M., Eds.) pp 441–468, Raven Press, Ltd, New York.

Kemble, G. W., Bodian, D. L., Rosé, J., Wilson, I. A., & White, J. M. (1992) *J. Virol. 66*, 4940–4950.

Korolkovas, A., & Burckhalter, J. H. (1976) *Essentials of Medicinal Chemistry*, John Wiley & Sons, New York.

Kuntz, I. D., Blaney, J. M., Oatley, S. J., Langridge, R., & Ferrin, T. E. (1982) *J. Mol. Biol. 161*, 269–288.

Maeda, T., Kawasaki, K., & Ohnishi, S.-I. (1981) *Proc. Natl. Acad. Sci. U.S.A. 78*, 4133–4137.

McSharry, J. J., Caliguiri, L. A., & Eggers, J. H. (1979) *Virology 97*, 307–315.

Morris, S. J., Sarkar, D. P., White, J. M., & Blumenthal, R. (1989) *J. Biol. Chem. 264*, 3972–3978.
Mosmann, T. (1983) *J. Immunol. Methods 65*, 55–63.
Otto, M. J., Fox, M. P., Fancher, M. J., Kuhrt, M. F., Diana, G. D., & McKinlay, M. A. (1985) *Antimicrob. Agents Chemother. 27*, 883–886.
Porter, R. F., Rees, W. W., Frauenglass, E., Wilgus, H. S., Nawn, G. H., Chiesa, P. P., & Gates, J. W. (1964) *J. Org. Chem. 29*, 588–594.
Presber, H. W., Schroeder, C., Hegenscheid, B., Heider, H., Reefschlager, J., & Rosenthal, H. A. (1984) *Acta Virol. 28*, 501–507.
Puri, A., Booy, F. P., Doms, R. W., White, J. M., & Blumenthal, R. (1990) *J. Virol. 64*, 3824–3832.
Richards, F. M. (1977) *Annu. Rev. Biophys. Bioeng. 6*, 151–176.
Rott, R., Orlich, M., Klenk, H.-D., Wang, M. L., Skehel, J. J., & Wiley, D. C. (1984) *EMBO J. 3*, 3329–3332.
Schroeder, C., Heider, H., Hegenscheid, G., Schoffel, M., Bubovich, V. I., & Rosenthal, H. A. (1985) *Antiviral Res. (Suppl. I)*, 95–99.
Shoichet, B. K., Bodian, D. L. & Kuntz, I. D. (1992) *J. Comput. Chem. 13*, 380–397.
Skehel, J. J., & Schild, G. C. (1971) *Virology 44*, 396–408.
Stegmann, T., Doms, R. W., & Helenius, A. (1989) *Annu. Rev. Biophys. Biophys. Chem. 18*, 187–211.
White, J. M. (1990) *Annu. Rev. Physiol. 52*, 675–697.
White, J. M., & Wilson, I. A. (1987) *J. Cell Biol. 105*, 2887–2896.
Wiley, D. C., & Skehel, J. J. (1987) *Annu. Rev. Biochem. 56*, 365–394.
Wilson, I. A., Skehel, J. J., & Wiley, D. C. (1981) *Nature 289*, 366–373.
Wireko, F. C., & Abraham, D. J. (1991) *Proc. Natl. Acad. Sci. U.S.A. 88*, 2209–2211.